

A New Numerical Method for Correction of Wide Gap Rheometry Data by CFD

Naser Hamed¹, Johan Revstedt¹, Eva Tornberg¹, and Fredrik Innings²¹ Lund University, Lund, Sweden.² Tetra Pak Processing System

ABSTRACT

In the present study an approach based on computational fluid dynamics (CFD) is used to find appropriate correction factors for rheometer data.

Two fluids, a mineral oil and Carboxyl Methyl Cellulose (CMC) 1.5% were used. Hence, both Newtonian and non-Newtonian effects are considered. CFD together with the integration approach was used to correct the measurement data and the calculated viscosity. The results of the wide and narrow gap rheometry were compared and the torque contribution for each part of the bob was specified. By the new approach, a correction factor for the end parts was found for narrow and wide gap measurement data. The results show that the correction factor to be larger for the wide gap. In addition, higher values of the correction factor were found for the non-Newtonian liquid. The CFD approach has a good potential of further improving the accuracy of rheological measurements.

INTRODUCTION

The Couette viscometer is widely used to measure the viscosity of the fluid. In order to keep the level of measurement uncertainty low, one normally aim at using as narrow gap as possible between the bob and the cup. However, for fibrous/particulate fluids where the size of the particles is relatively large, a wider gap

must be used. The flow of a Newtonian fluid will then deviate more from the classical Taylor-Couette solution and, hence, the shear rate distribution over the gap is not known a priori. This longstanding problem in rheometry is often referred to as the “Couette Inverse Problem”¹. To solve this problem, the flow curve is derived from the measurement data obtained by the experiment. Note that the terms narrow and wide should not be interpreted in an absolute sense, but rather as relative quantities, i.e. the distance between the rotating bob and the stationary cup in relation to the height of the bob.

Several methods have been proposed to solve this problem. A widely used method is based on the analytical solution of the governing equations and is the “integration approach”². Other approaches are mainly based on numerical solution of the ill-posed integral in Eq. 1³:

$$\omega = \int_{R_i}^{R_o} \frac{\dot{\gamma}}{r} dr \quad (1)$$

In Eq 1, R_o and R_i are the outer and inner radius of the cup and bob, respectively. ω is the rotational speed and $\dot{\gamma}$ is the shear rate.

There are studies addressing the solution of the Couette inverse problem based on the solution of Eq. 1. To extract $\dot{\gamma}$ from Eq. 1, the integral should be inverted. This integral inversion is the source of the problem in the

wide gap rheometry. To solve it, numerical differentiation should be carried out on the noisy experimental data which requires selecting suitable algorithm⁴. Among the numerical methods used to achieve this, one may mention the method by Yeo et al.⁵ based on Tikhonov regularization and the wavelet-veguelette decomposition method by Ancey⁶. One may also employ experimental methods in order to find proper coefficients for the measurement correction. Barnes⁷, for example, proposed an experimental method to correct the wide-gap viscometry data based on the narrow-gap approximation.

Neglecting the end effects one may directly relate the shear stress on the bob-surface to the torque (T):

$$\tau = \frac{T}{2\pi h R_i^2} \quad (2)$$

where h is the bob height.

However, the shear stress on the end surfaces will also contribute to the measured torque. Based on Eq. 2, Nguyen and Boger⁸ proposed a method for calculating the shear stress on the cylindrical surface accounting for the shear stress on the end surfaces. As a first approximation they assumed that the end surface shear stress is evenly distributed and equal to the shear stress on the cylindrical surface:

$$\tau = T \frac{1}{2\pi R_i^3} \left(\frac{h}{R_i} + \frac{2}{3} \right)^{-1} \quad (3)$$

By solving Eq. 1 and using Eq. 2 and the linear relation between shear rate and shear stress for a Newtonian fluid one may relate the shear rate to the angular velocity of the bob, as has been shown by for example Steffe⁹:

$$\dot{\gamma} = - \frac{2\omega R_o^2}{(R_i^2 - R_o^2)} \quad (4)$$

In Eq. 4, the effects of the end parts of the bob are neglected.

The aim of the present work is to develop a method, based on computational fluid dynamics (CFD), to find a correction factor that will in combination with the integration approach improve the accuracy of wide gap rheometer data.

Furthermore, we aim to quantify the torque contribution from the end surfaces and how this is influenced by the width of rheometer gap, and the power law index of the fluid.

The dimensions of the wide gap rheometer are $R_o=13.75\text{mm}$, $R_i=7\text{mm}$, $h_{\text{bob}}=21\text{mm}$ and $h_{\text{cup}}=62.5\text{mm}$. For the narrow gap the bob dimensions are $R_i=12.5\text{mm}$, $h_{\text{bob}}=37.5\text{mm}$ and the same cup.

MATHEMATICAL FORMULATIONS

The description below is based on the assumptions that the flow is steady, laminar and without secondary motion, which is indeed the case considering the very low Reynolds and Taylor numbers. Considering the modelling of the non-Newtonian fluid used, the power law behaviour is only valid in a certain range of shear rates. Hence, to as accurately as possible model the flow of CMC and to avoid numerical difficulties at very low shear rates a constant viscosity was applied below a certain value of $\dot{\gamma}$. Finally, the estimation of the flow properties namely the ‘‘power law index’’ (n) and the viscosity/consistency index (m) is crucial and sensitive to the existing noise in the experimental data. Therefore, a local averaging method was applied to reduce the noise before calculating m and n.

Eq. 5 and Eq. 6 are the result of solving Eq. 1 using Eq. 2 to relate the torque to the shear stress, i.e. what is here denoted as the integration approach, for Newtonian and power-law fluids, respectively. Power-law index (n) is calculated as $n = \frac{d \ln T}{d \ln \omega}$ and the

consistency index (m) could be calculated afterwards. ω is the rotational speed in rad/s.

$$T = \frac{4\mu\pi h}{(1/R_i^2 - 1/R_o^2)} \omega \quad (5)$$

$$T = \frac{2^{n+1}\pi h}{n^n \left(\frac{1}{R_i^{2/n}} - \frac{1}{R_o^{2/n}} \right)} m \omega^n \quad (6)$$

μ (Pa.s) is the viscosity in Newtonian fluids in Eq. 5.

From Eq. 5 and Eq. 6, one can define

$$C = \frac{4\pi h}{\left(\frac{1}{R_i^2} - \frac{1}{R_o^2} \right)} \quad \text{and} \quad C = \frac{2^{n+1}\pi h}{n^n \left(\frac{1}{R_i^{2/n}} - \frac{1}{R_o^{2/n}} \right)} \quad \text{as the}$$

coefficients, which are used to extract the fluid properties in the wide gap rheometry in Newtonian and non-Newtonian fluids, respectively. For further details on this, see Steffe⁹.

In the present method, the integration approach is used to get a first estimate of the viscosity. This value is then introduced into the CFD model.

The coefficient C using Newtonian fluids has a unique value for every experimental set-up, i.e. it is only dependent on the geometry of the measuring unit. For non-Newtonian fluids it also depends on the power-law index which means that for every rheometer and for every non-Newtonian fluid, a correction factor must be calculated, which is usually neglected in the measurements activities.

NUMERICAL MODEL

A 30° slice of the three dimensional (3-D) model was considered as the computational domain, Fig. 1a.

The simulations were performed on a structured hexahedral mesh using ANSYS CFX 14 (ANSYS Inc., Canonsburg, PA). A periodic boundary condition was used for the side surfaces and for all solid surfaces no-slip conditions are used. The pressure reference point was placed at the top cup side.

Fig. 1b shows the result of the grid sensitivity study using the computational domain for wide gap model. X-axis represents the number of grids across the gap and Y-axis denotes the measured CFD torque. As can be seen, there are only minor differences in the torque for the three finest grid resolutions. The same series of simulations were performed for narrow gap numerical model for $\omega=1$ rad/s.

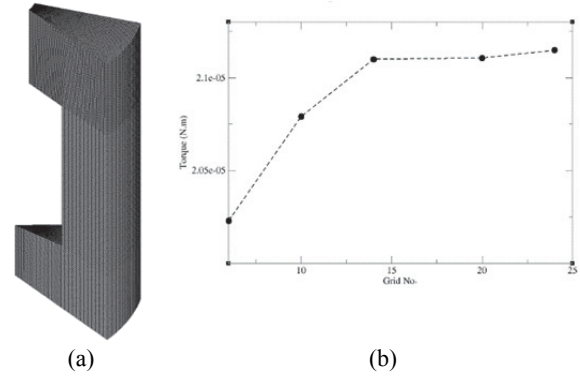


Figure 1. 1a) Discretized wide gap model, 1b) Calculated torque for several grid resolutions.

EXPERIMENTAL SETUP

The experiments were performed in two series measuring the rheological properties of Newtonian and non-Newtonian fluids. A mineral oil is selected as the Newtonian fluid and Carbon Methyl Cellulose (CMC) 1.5% is selected as the non-Newtonian fluid. The experiments were examined in Kinexus® rotational rheometer (Malvern Instrument Ltd., Malvern, UK) with both narrow and wide gap bobs.

RESULTS AND DISCUSSION

Shear rate distribution

Fig. 2 shows the shear rate distribution in the wide and narrow gap rheometry for a Newtonian fluid. As shown in Fig. 2, the shear rate clearly changes along the wide gap while in the narrow gap less variation can be observed. We expected to have a variation in the shear rate distribution in the

wide gap, but in the narrow gap the effect of the top and bottom parts on the shear rate was observed, too. This is shown by the small shear rate zones on the bob ends in both gaps and a slight difference between the shear rate values on the bob-face and the cup.

As is evident from Fig. 2b, in the wide gap, the shear rate changes along the wide gap height while in the narrow gap, it is approximately constant over the height.

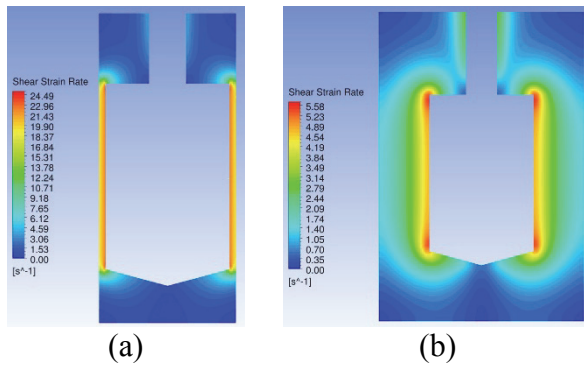


Figure 2. Shear rate distribution in narrow (left) and wide (right) gaps for a Newtonian fluid (Note that the color maps differ in the two cases.)

The concentrated shear rate that is shown in the bottom and the top corners of the bob-face in the wide gap increases the non-linearity of the shear rate distribution across the gap especially in the regions closed to the end parts. As is seen in Fig. 2, the rod also has some effect on the overall shear rate.

Torque contribution

The torque contribution for different parts of the bob is shown in Table 1 for wide and narrow gap and for Newtonian and non-Newtonian liquids, respectively. For Newtonian fluids, the contribution of the different parts of the bob is constant for different rotational speeds and viscosities as it is only the function of the dimensions of the bob. For non-Newtonian fluid, it is also dependent to the power-law index (n).

Table 1. Relative contribution to the torque, in percentage, of the different parts of the bob.

	Gap	bottom	top	face	rod
Oil	narrow	3.4	2.7	93.5	0.4
	wide	6.7	5.9	85.5	2.0
CMC	narrow	6.2	5.1	87.4	1.4
	wide	8.0	6.8	82.2	3.0

Comparing narrow and wide gap rheometry results for Newtonian fluids in Table 1, one finds that the relative contribution from the end surfaces is about twice as large in the wide gap case.

As expected, the bottom end contributes more to the torque in both Newtonian and non-Newtonian cases than the top and the rod. Although there is a gap between the bob bottom tip and the cup end (which is called “zero-gap” in rheometry), this closed area increases the contribution in the required torque due to the bottom wall effects. Moreover, the bottom surface has larger area than the top ones.

For the non-Newtonian fluids, the end part torque contribution is more pronounced than in the Newtonian cases. This fact will be discussed later.

It is note-worthy that the shear rate gradient in the non-Newtonian cases is more pronounced than for the Newtonian fluids due to the high non-linearity of the equations in non-Newtonian flow. Figs. 3 and 4, show how the shear rate changes across the narrow and wide gap in Newtonian and non-Newtonian cases. The rotational speeds are equal in the two cases.

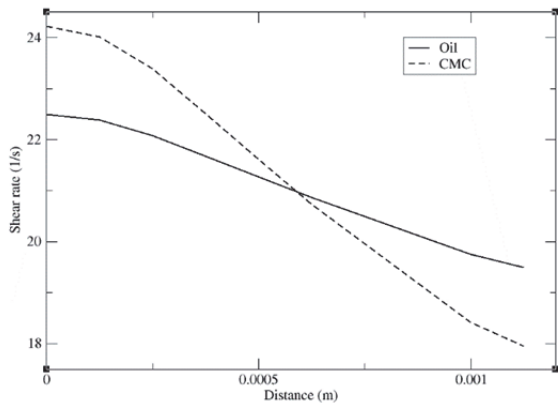


Figure 3. Shear rate profile along the narrow gap.

Non-linearity of the velocity profile in non-Newtonian narrow gap cases is shown in Fig. 5.

In the wide gap rheometry, the shear rate and the velocity show non-linear behaviour, see Figs. 4 and 6.

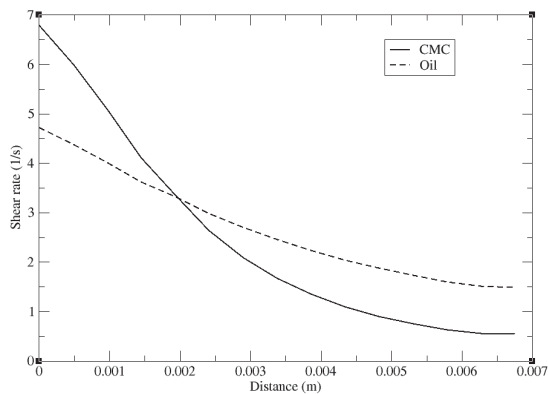


Figure 4. Shear rate profile along the wide gap.

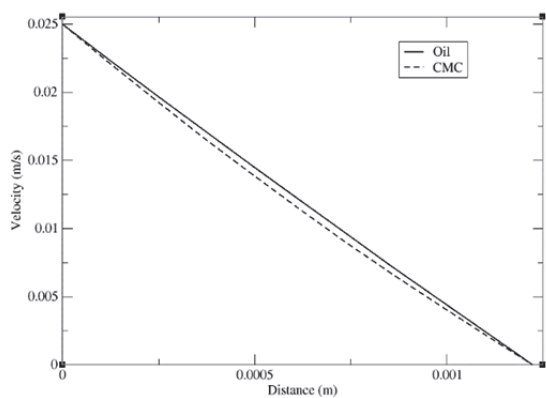


Figure 5. Velocity profile along the narrow gap.

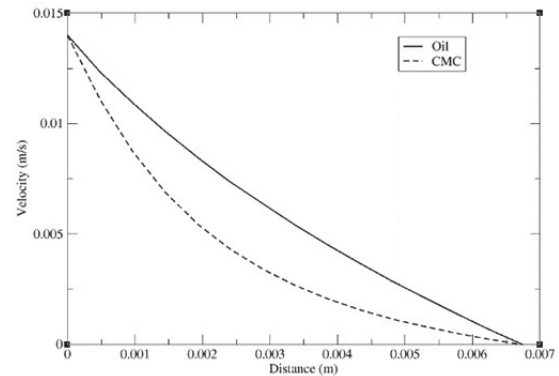


Figure 6. Velocity profile along the wide gap.

According to Eq. 6, the torque for a power-law fluid is also dependent on the power-law index (n). Fig. 7 and Fig. 8 show how the torque contribution in different parts changes with the power-law index. Torque contribution for the bob-face is increased as the shear thinning of the fluid is decreased.

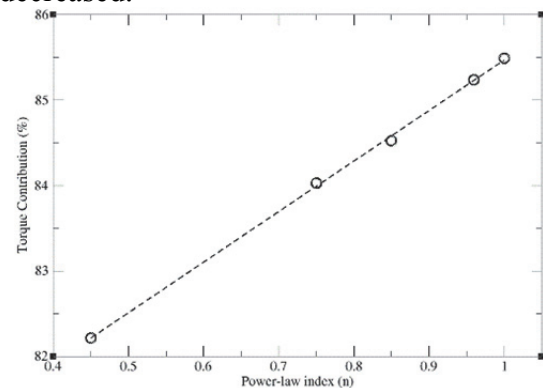


Figure 7. Torque contribution by the bob-face as a function of power-law index.

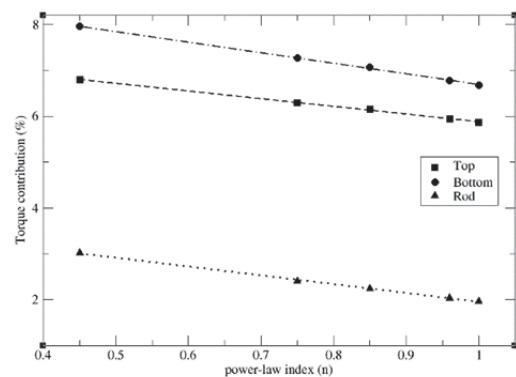


Figure 8. Changes of the contribution of the torque by the end parts as a function of power-law index.

Correction

The C factors by the integration approach neglects the end effects on the torque. By the CFD approach we can calculate the C factor more precisely. The factor (C) can be split into two different factors, C_g and C_e . C_g is equivalent to the geometrical factor in the integration approach and C_e is the end effect correction factor, which are calculated by the CFD approach.

$$T = C_g \cdot C_e \cdot \mu \cdot \omega$$

$$T = C_g \cdot C_e \cdot m \cdot \omega^n$$

Tables 2 shows the corresponding values for correction factors for Newtonian and non-Newtonian fluids using the CFD approach.

Table 2. Correction factors from CFD approach

Fluid	Oil		CMC	
	Narrow	Wide	Narrow	Wide
C_e	1.09	1.27	1.17	1.31

From Table 2, it is observed that the end correction factor is increased going from a narrow to a wide gap and from Newtonian to non-Newtonian rheometry measurements. Hence, the largest end correction factor is found in wide gap rheometry of the CMC, which is consistent with the results shown in Table 1. The values of C_e using the approach by Nguyen and Boger⁸ are only dependent on the ratio between the bob radius and the bob height. The end effect correction can then be written in accordance with Nguyen and Boger⁸ as:

$$C_e = \frac{R_i}{h} \left(\frac{h}{R_i} + \frac{2}{3} \right) \quad (12)$$

As the ratio of the bob radius to the bob height is equal to 1/3 in the cases presented here, which follows the recommended values in the DIN Standard¹⁰, the value of C_e is 1.22 in both narrow and wide bob.

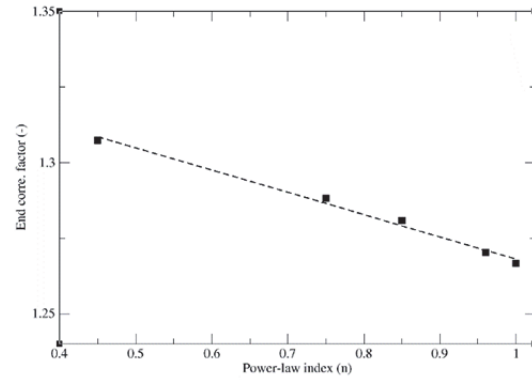


Figure 9. End correction factor variation with power-law index (n)

Fig. 9 shows how C_e varies with power-law index for the CFD correction method for wide gap rheometry. As the effect of the end parts increases with enhanced shear thinning properties of the fluid, the corresponding correction factor gets larger.

The resulting fluid properties are shown in Tables 3-5.

Table 3. Viscosity values for the Newtonian cases

Fluid	Integration App.		CFD App.	
	Narrow	Wide	Narrow	Wide
μ	1.02	1.18	0.94	0.94

Table 4. Flow curve values for the non-Newtonian case

Fluid	Integration App.		CFD App.	
	Narrow	Wide	Narrow	Wide
m	12.19	15.92	10.25	12.08
n	0.46	0.45	0.46	0.45

Table 5. Viscosity values using the end effect correction by Nguyen and Bolger⁸ for the Newtonian fluid

Fluid	Oil	
	Narrow	Wide
μ	0.83	0.97

From Table 3, it is evident that the integration approach overestimates the viscosity values since it neglects the influence of the end parts. A similar trend is found for the non-Newtonian fluid in table

4. Comparing the results of the integration approach and CFD method to the Nguyen and Bolger⁸, it is clear that the wide gap results are significantly improved. However, for the narrow gap the method by Nguyen and Bolger⁸ overestimates the end effects.

CONCLUSIONS

A series of experiments and numerical simulations were performed to find a more precise correction procedure for Couette rheometry measurements. By using CFD the flow fields were mapped in narrow and wide gap for Newtonian and non-Newtonian fluids.

Traditional correction procedures usually neglects the effects of the end parts on the inverse calculation of the flow properties. CFD has the potential to investigate the flow field details and to understand the physics of the problem. The integration approach combined with the CFD calculation was used to find the correction coefficients.

The torque contribution for different parts of the bob was estimated in both narrow and wide gaps. Narrow gap rheometry is widely accepted as a reference for the fluid properties while our CFD calculations showed that there is also a significant error in non-Newtonian narrow gap rheometry due to the end effects. The end part torque contributions are largely increased for the non-Newtonian liquids. Moreover, the shear rate distribution and the velocity profile along the gap for the non-Newtonian fluid are highly non-linear in the wide gap rheometry. A slight non-linearity of velocity profile was observed in narrow gap shear thinning rheometry.

For the different shear thinning fluids, the torque contribution was calculated. The correction factor for the end parts (C_e) was calculated for some shear thinning liquids. Higher shear thinning fluids rheometry need higher values of the end correction factor.

The integration approach overestimate the flow curve properties. Applying the

CFD correction approach highlights the end effects and precisely predict the fluid properties.

The CFD approach is shown to be a useful tool to calculate the correction factor in Couette viscometer in both Newtonian and power law fluids.

ACKNOWLEDGMENTS

The authors would like to acknowledge Tetra Pak and Tvärilivs to financially support the project. The simulations were performed on resources provided by the Swedish National Infrastructure for Computing (SNIC) at the Center for scientific and technical computing at Lund University (LUNARC).

REFERENCES

1. Kirsch, A., an Introduction to Mathematical Theory of Inverse Problems, Springer, New York, 1996.
2. G. Heirman et al., Integration Approach of Couette Inverse Problem of Powder Type Self-Compacting Concrete in a Wide Gap Concentric Cylinder Rheometer, *J. Non-Newtonian Fluid Mech.*, 150 (2008) 93-103.
3. Friedrich, C., New ill-posed problems in rheology, *Rheol Acta* 35:186-193 (1996).
4. Christian Friedrich, Josef Honerkamp, Jfirgen Weese, New ill-posed problems in rheology, *Rheol Acta* 35:186-193 (1996).
5. Yeow, Y., Ko, W., Tang, P., Solving the inverse problem of Couette viscometry by Tikhonov regularization, *J. Rheol.* 44 (2000) 1335–1351.
6. C. Ancey, Solving the Couette inverse problem using a wavelet–vaguelette decomposition, *J. Rheol.* 49 (2005) 441–460.
7. H.A. Barnes, *A Handbook of Elementary Rheology*, Institute of Non-Newtonian Fluid

Mechanics, University of Wales, pp (49), 2000.

8. Nguyen Quoc Dzuc and D. V. Boger, Yield Stress Measurement for Concentrated Suspensions, *Journal of rheology*, 27 (4), 321-349 (1983).

9. James F. Steffe, *Rheological methods in Food Process Engineering*, Freeman press, (1996).

10. DIN 53019-3: 2008-09, Measurement of the viscosities and flow curves by means of rotational viscometers, part3: measurement errors and corrections.